

## Article

### Pulsed Magnetic Field Induced Fast Drug Release from Magneto Liposomes via Ultrasound Generation

George Podaru, Raj Dani, Hongwang Wang, Matthew Thomas  
Basel, Punit Prakash, Stefan H. Bossmann, and Viktor Chikan

*J. Phys. Chem. B*, Just Accepted Manuscript • DOI: 10.1021/jp5022278 • Publication Date (Web): 11 Aug 2014

Downloaded from <http://pubs.acs.org> on August 23, 2014

#### Just Accepted

"Just Accepted" manuscripts have been peer-reviewed and accepted for publication. They are posted online prior to technical editing, formatting for publication and author proofing. The American Chemical Society provides "Just Accepted" as a free service to the research community to expedite the dissemination of scientific material as soon as possible after acceptance. "Just Accepted" manuscripts appear in full in PDF format accompanied by an HTML abstract. "Just Accepted" manuscripts have been fully peer reviewed, but should not be considered the official version of record. They are accessible to all readers and citable by the Digital Object Identifier (DOI®). "Just Accepted" is an optional service offered to authors. Therefore, the "Just Accepted" Web site may not include all articles that will be published in the journal. After a manuscript is technically edited and formatted, it will be removed from the "Just Accepted" Web site and published as an ASAP article. Note that technical editing may introduce minor changes to the manuscript text and/or graphics which could affect content, and all legal disclaimers and ethical guidelines that apply to the journal pertain. ACS cannot be held responsible for errors or consequences arising from the use of information contained in these "Just Accepted" manuscripts.



ACS Publications

High quality. High impact.

The Journal of Physical Chemistry B is published by the American Chemical Society.

1155 Sixteenth Street N.W., Washington, DC 20036

Published by American Chemical Society. Copyright © American Chemical Society.

However, no copyright claim is made to original U.S. Government works, or works produced by employees of any Commonwealth realm Crown government in the course of their duties.

# Pulsed Magnetic Field Induced Fast Drug Release from Magneto Liposomes via Ultrasound Generation

George Podaru, Raj Kumar Dani, Hongwang Wang, Matthew T. Basel, Punit Prakash, Stefan H. Bossmann, \*Viktor Chikan

Department of Chemistry, Kansas State University, Manhattan, KS 66502

Department of Electrical Engineering, Kansas State University, Manhattan, KS 66502

†Department of Chemistry, University of Kansas, Lawrence, KS 66045

\*Corresponding author. vchikan@ksu.edu, (785)532-6807

## Abstract

Fast drug delivery is very important to utilize drug molecules that are short lived under physiological conditions. Techniques that can release model molecules under physiological conditions could play an important role to discover the pharmacokinetics of short lived substances in the body. Here an experimental method is developed for the fast release of the liposomes' payload without a significant increase in (local) temperatures. This goal is achieved by using short magnetic pulses to disrupt the lipid bilayer of liposomes loaded with magnetic nanoparticles. The drug release has been tested by two independent assays. The first assay relies on the AC impedance measurements of MgSO<sub>4</sub> released from the magnetic liposomes. The second standard release assay is based on the increase of the fluorescence signal from 5(6)-Carboxyfluorescein dye when it the dye is released from the magneto liposomes. The efficiency of drug release ranges from a few percent to up to 40% in case of the MgSO<sub>4</sub>. The experiments also indicate that the magnetic nanoparticle generate ultrasound, which is assumed to have a role in the release of the model drugs from the magneto liposomes.

**KEYWORDS:** liposomes, drug delivery, magneto-liposomes, magnetic nanoparticles, ultrasound

### Introduction

Liposomes were first described in 1961 (published 1964<sup>1</sup>) by Alec Bangham. Liposomes (and the payload that they have trapped inside during formation), can be separated from smaller molecules simply by gel filtration or dialysis, making them very useful delivery agents.<sup>2, 3</sup> Liposomes are stable in blood, not releasing their contents,<sup>2, 4, 5, 6</sup> and when incubated with plasma constituents, they retain their spherical shape.<sup>7, 8</sup> Liposomes made from L,  $\alpha$ -dipalmitoylphosphatidylcholine (DPPC) are widely used for the intravenous delivery of drugs, because they are not prohibitively expensive and feature suitable biophysical properties. The higher phase transition temperature ( $T_m$ ) of DPPC is 314K. At  $T > T_m$  liposomes can be filtered through porous membrane filters, which makes spherical unilamellar liposomes with a very small polydispersity available.<sup>9</sup> The fast removal of the liposomes by the macrophages and monocytes of the reticuloendothelial system can be prevented by attaching a polyethylene glycol coating to the outside of the liposome.<sup>10</sup> Polyethylene glycol apparently creates a steric block around the outside of the liposome that does not interact with recognition molecules. Since the polyethylene glycol does not interact with recognition molecules and it prevents the recognition molecules from reaching the liposomal surface, the liposomes are widely ignored by the reticuloendothelial system. The liposomes prepared this way(liposomes coated in polyethylene glycol) have come to be known as stealth liposomes.<sup>10</sup>

To date, several liposomal drug delivery systems have been developed (e.g. Nicoderm and others)<sup>11, 12</sup> that rely on the slow release of their payload. However, for the treatment of cancer or infectious diseases, it is certainly desirable to deliver the payload (drug) at once after the target has been reached. Several research groups have used AC-magnetic hyperthermia to trigger the release of magnetoliposomes' payload by heating magnetic nanoparticles within the supramolecular nanostructure until they either burst or (partially) dissolve in the surrounding aqueous medium.<sup>13</sup> Although this approach appears to work, it has the disadvantage that the liposomes' payload may be damaged by the heat and the release is not instantaneous. This is certainly valid for anticancer drugs like SN-38 and its prodrug irinotecan<sup>14</sup> and si-RNA<sup>15</sup> that can degenerate when heated above  $T=330K$ . The release of drugs also takes place on a minutes time scale.

Here a method is developed for the immediate release of the liposomes' payload without a significant increase in (local) temperatures. This goal is achieved by using the mechanical

1  
2  
3 motion of magnetic nanostructures that are embedded within either the cores or the lipid bilayers  
4 of the liposomes, or at the interface between core and bilayer. The mechanical stimulus is  
5 induced by the application of a strong magnetic pulse. The liposomes are used here feature  
6 comparatively low diffusion coefficients. Without an external stimulus, they will retain their  
7 payload for extended periods of time.<sup>16</sup> To meet this challenge, the cholesterol content of their  
8 lipid bilayers is adjusted. The mechanical motion of the magnetic nanoparticles locally  
9 destabilizes the lipid bilayer and causes its collapse and the subsequent release of the liposomes'  
10 payload. In contrast to the heat induced release of drug from magneto liposomes from AC  
11 magnetic fields, the drug release is takes place due to mechanical motion of magnetic  
12 nanoparticles therefore produce significantly less amount of residual heating. The successful  
13 application of the mechanical force of the nanoparticles to create controlled disruption in a lipid  
14 bilayer places some limits on the nanoparticles and magnetic fields that can be used in the  
15 experiments.

16  
17  
18  
19  
20  
21  
22  
**Experimental Section:**  
23  
24  
25

26  
27  
28  
**Construction of pulsed electromagnet for drug release studies**  
29  
30

31 In 1924, the first pulsed magnetic field, close to 50 T, was developed by P. Kapitza from his lead  
32 acid storage battery through 1 mm bore and he was optimistic about obtaining 200-300 T if  
33 adequate financial means became available.<sup>17</sup> Pulsed magnets are used for two reasons: they can  
34 provide the highest fields and they can be made to fit a moderate budget. The generation of  
35 pulsed magnetic field is important for several activities in the area of physical sciences. The  
36 basic components of a pulsed magnetic field are capacitor bank (C), power supply (V), spark gap  
37 (also called thyratron switch), inductor (L) and resistors (R). Basically, a pulsed magnetic field  
38 circuit is RLC (Resistor – Inductor – Capacitor) circuit. A simple schematic diagram for the  
39 pulsed magnetic field is shown in the Figure 1.  
40  
41  
42  
43  
44  
45  
46  
47  
48  
49  
50  
51  
52  
53  
54  
55  
56  
57  
58  
59  
60

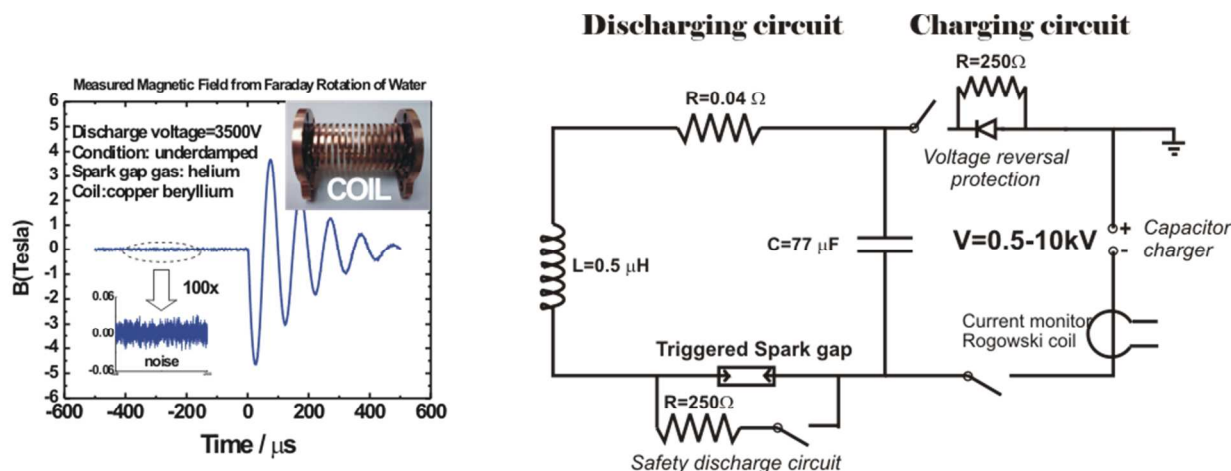


Figure 1 LEFT Experimentally determined pulse magnetic field from Faraday rotation of water. The inset shows the picture of the helical beryllium copper coil used in the experiments Schematic circuit diagram of the pulsed magnetic field apparatus.

The capacitor bank is charged with a power supply. When the charged capacitor bank is discharged through the inductive coils for a short time, electric energy is transformed into magnetic energy.<sup>18</sup> The production of suitable shaped magnetic field requires a current to pass through a coil, but choosing the parameters of the coil is nontrivial because of trade-off between the magnetic field strength, the field homogeneity, and the inductance of the coil. Increasing the number of turns of the coil increases the field strength for a given current and increasing the diameter of the coil provides a larger region of the field uniformity but decreases the field strength. An increase in either the coil diameter or number of turns causes an increase in the inductance of the coil, and so for maximizing the rate of field switching, the number of turns and coil diameter should be minimized.<sup>19</sup> A series of resistors controls the charging current. The value of  $\pi\sqrt{LC}$  gives the duration of the pulse.<sup>20</sup> The pulsed magnet constructed for this work consists of a capacitor bank of 77.3  $\mu$ F of Maxwell Laboratories which is charged by a power supply/charger of Lumina Power, Inc. The power supply uses 100-240 V AC-50/60 Hz input and output of 10kV@500 J/s in continuous operation. All the experimental operations are controlled by the computer programmable controller. The overall discharge energy can be calculated using the expression  $\frac{1}{2} CV^2$ . Principally, the discharge of the capacitor bank to be critically damped which implies  $R = 2 \sqrt{L/C}$ . The spark gap is the major resistance in the circuit, and most of the energy is dissipated through the spark gap during discharge and the remaining, negligible, energy is used in the Joule heating of the circuit.<sup>20</sup> A small spark gap gives the necessary resistance for the critical damping. Theoretically, the capacitor bank needs to be charged to cross the

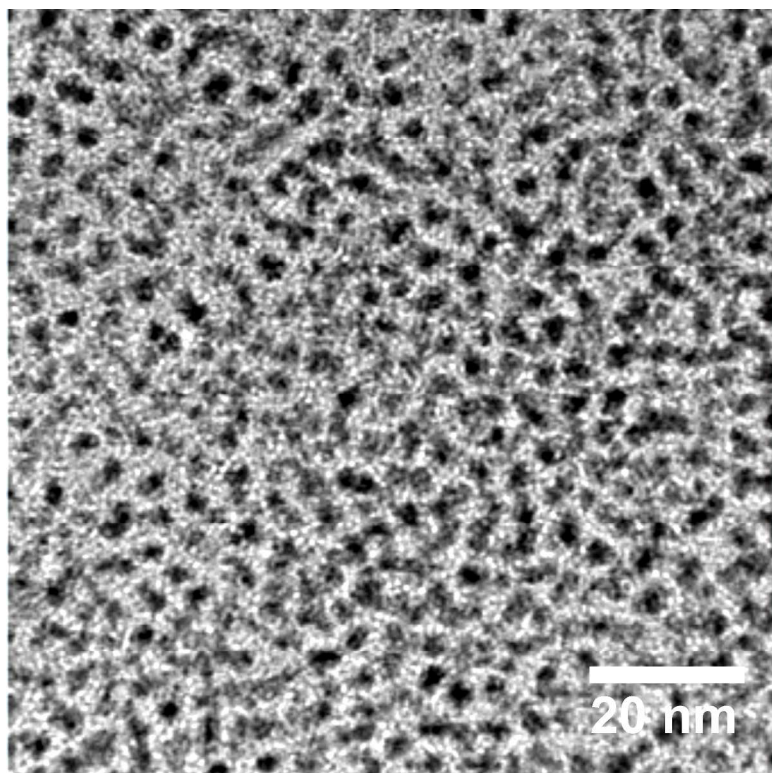
breakdown voltage of the spark gap. The breakdown voltage is the minimum voltage that causes a portion of insulator to become electrically conductive and complete the electric circuit. In these experiments the spark gap is fixed to approximately 2 mm and is triggered by using a high voltage trigger pulse generator.

The strength of the magnetic field applicator is measured via the Faraday rotation of an optical material with known optical constant.<sup>20</sup> The strong magnetic field induces birefringence of an optical material rotate the plane of polarization of a linearly polarized light proportional to the amount of magnetic field according to  $\theta = vBl$  where  $v$  is Verdet constant of the material,  $B$  is the magnetic field and  $l$  is the optical path length. The magnitude of Faraday rotation of optical materials is linearly proportional to the amount of magnetic field, which is utilized in calibration the pulsed magnetic field for the experiments described in this paper. For the calibration of magnetic fields, either borosilicate glass or water is used with known optical pathlength. The Faraday rotation constant (Verdet constant) of these materials are published in the literature. A linearly polarized 632 nm HeNe laser is passed through the water or borosilicate glass sample. The exiting laser beam passes through an analyzer (calcite prism ) oriented 45° relative to the orientation of the linear polarized light, which allows splitting the laser into two equal intensity beam that are projected on a balanced photodiode (Model 2307 Large-Area Adjustable-Gain Balanced Photoreceivers from Newport Inc.). The photoreceiver is placed far from the magnetic field to minimize any electronic interference from magnetic fields directly influencing signal on the photoreceivers. When the magnetic field is present, the rotation of magnetic field appears as positive or negative signal (depending on the direction of the magnetic field) on the oscilloscope from the balanced photodiode. Based the characteristics of the photoreciever, the optical power difference and the magnitude and direction of the Faraday rotation signal is calculated. Comparing the measured signal with the value from the faraday equation of the material, the magnetic field is calculated. For the drug release studies, the peak strength of the magnetic pulse remained at approximately 3 Tesla. The actual magnetic field profile from faraday measurement is shown in the inset of Figure 7.

### **Synthesis of magnetic nanoparticles**

The PtFe nanoparticles (Figure 2) are synthesized via the following procedure described by Chao Wang et all.<sup>21</sup> 0.015 moles of oleylamine and 0.015 moles of octadecene and 0.00025 moles of platinum(II)acetylacetone (Pt(acac)<sub>2</sub>) is loaded into a 3 neck round bottom flask. This flask is

1  
2  
3 purged vacuumed and backfilled with argon gas three times and temperature is raised to 60 °C.  
4 The solution is allowed to sit there for 10 min and then quickly heated (in less than 5 min) to 120  
5 °C. Upon reaching 120 °C, 0.00025 moles of iron pentacarbonyl is rapidly injected into the flask  
6 and the temperature was raised to 160 °C and allowed to sit at this temperature for 30 min.  
7 Particles are then allowed to cool to room temperature and were cleaned using standard  
8 centrifugation (rinse 3 times hexane/ethanol) and re-dissolved in hexane.  
9  
10  
11  
12  
13



41 **Figure 2 FePt nanoparticles used in the experiments**  
42  
43

44 Iron nanoparticles were prepared with slight modification of a literature procedure  
45 described by Lacroix et al.<sup>22</sup> A 250 mL, three-necked, round-bottom flask equipped with a  
46 magnetic stir bar, one cold water cooled jacket condenser on the middle neck, one septum and  
47 one temperature probe on each of the outer necks is charged with 60 mL 1-octadecene (ODE),  
48 0.9 mL oleylamine and 0.831 g hexadecylammonium chloride (HAD.HCl). The reaction system  
49 is connected to a Schlenk line through the top of the jacket condenser. The reaction mixture is  
50 degassed at 120 °C for 30 min with vigorous stirring. After refilled with argon, the reaction  
51 mixture is heated to 180 °C. Three portions of 0.7 mL Fe(CO)<sub>5</sub> are injected into the reaction  
52  
53  
54  
55  
56  
57  
58  
59  
60

mixture via a syringe in every 20 min. The reaction mixture is kept at 180 °C for another 20 min after the last injection, and cooled to room temperature naturally. The supernatant is decanted, and the iron nanoparticles accumulated on the magnetic stir bar are washed with hexane and ethanol. The product is dried in vacuum and stored at room temperature for further use. Based on iron, the yield of the reaction is 95%.

Three coatings of Fe/Fe<sub>3</sub>O<sub>4</sub> will be used by attaching either hydrophilic, amphiphilic or hydrophobic peptide sequences. HIV-1 Tat-(48-60) (GRKKRRQRRRPPQ) will serve as the hydrophilic oligopeptide.<sup>44</sup> In its monomeric form, it is known to bind to double-layers.<sup>45</sup> Penetratin will be employed as the amphiphilic oligopeptide (RQIKIWFQNRRMKWKK)<sup>46</sup> and Membrane Translocating Sequence Peptide (AAVALLPAVLLALLP)<sup>47</sup> will be used as the hydrophobic oligopeptide.

Core/shell magnetic Fe/Fe<sub>3</sub>O<sub>4</sub> nanoparticles were first coated with dopamine, and through which, free NH<sub>2</sub> groups were introduced into the surface of nanoparticles (See Figure 3). Next, reacting the C-terminal of hydrophilic, amphiphilic or hydrophobic peptide sequences with the NH<sub>2</sub> groups resulted in the peptide functionalized magnetic nanoparticles. Briefly, 10 mg of dopamine coated Fe/Fe<sub>3</sub>O<sub>4</sub> nanoparticles were dispersed into 2 mL of dry DMF, 5 mg of peptide sequence, 0.6 mg of EDC, 0.3 mg of DMAP were added to the suspension sequentially. After brief sonication, the reaction mixture was swirled vigorously at room temperature for 12 hours. MNPs were collected by centrifugation (10000 rpm, 5min), and washed with DMF (2mL × 3 times), methanol (2mL × 3 times). The MNPs were finally dried under vacuum, and stored under Argon for liposome loading.

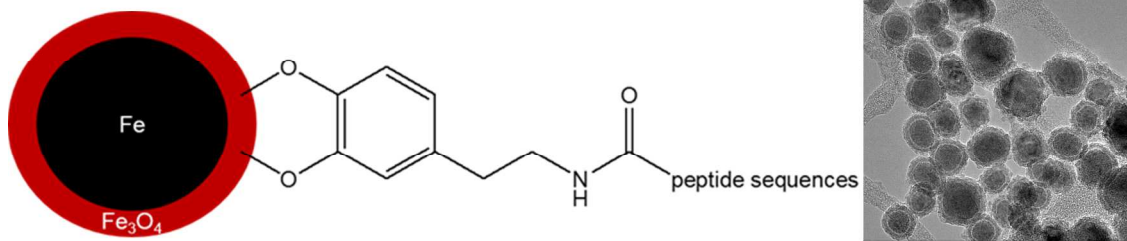


Figure 3 LEFT Schematic view of the Iron oxide nanoparticles coatings for the release studies presented in this manuscript. The peptide sequence modification allows modifying the hydrophobicity of the nanoparticle coating. RIGTH TEM image of Core/shell magnetic Fe/Fe<sub>3</sub>O<sub>4</sub> nanoparticles

The commercial 10 nm iron oxide nanoparticles used in the ultrasound studies were purchased from Ferrotec EMG Series, and they are water-based ferrofluid type EMG 607 stabilized with cationic surfactant.

### **Magneto liposome preparation and characterization**

Liposomes are produced by the thin-film hydration method coupled with sequential extrusion method which is adopted from the Ph.D. thesis of Matthew T. Basel.<sup>23</sup> To prepare magneto liposomes (Figure 4) 88:1:10 molar ratio of 1,2-dipalmitoyl-sn-glycero-3-phosphocholine (DPPC), 1,2-distearoyl-sn-glycero-3-phosphocholine (DSPC) and cholesterol are mixed for total lipid 10 mg in a round-bottom flask. Then, in order to ensure a homogeneous mixture of the lipids is dissolved in an organic solvent (chloroform). The solution was then vortexed for one minute to ensure the even dispersion of the lipids and cholesterol. DSPC and DPPC are the phospholipids used to create the lipid bilayer of the liposomes, and cholesterol is added for increased stability. Once these compounds have been added, the chloroform is evaporated off at approximately 55°C. After evaporating the chloroform, the sample is placed in vacuum for one hour. The next step is hydration of the thin-film lipid which is carried out simply by adding and agitating an aqueous medium into the thin-film of the lipids. Next, the residue is hydrolyzed in which either with 125 microliters of Phosphate Buffered Saline (0.136 M NaCl, 0.0045 M KCl, 0.012 M PO<sub>4</sub><sup>3-</sup> buffered to pH 7.4) or 125 microliters of HEPES Buffered Saline (0.136 M NaCl, 0.0045 M KCl, 0.012 M HEPES buffered to pH 7.4), together with 838 microliters of double distilled water, 37 microliters of 3M NaOH are added to the dried phospholipids. During this step, the encapsulation of a defined amount of nanoparticle solution (FePt or Fe/Fe<sub>3</sub>O<sub>4</sub>), MgSO<sub>4</sub> (25 mg) and carboxyfluorescein (25 mg) occurs simply by adding the desired amount to the lipid solution. If the nanoparticles are insoluble in water, one should mix them with lipid before making thin film of lipid. For the control experiments the same protocol was used, the only difference being the fact that no nanoparticles were added. After everything has been added to the lipid/nanoparticle solution, the mixture is vortexed the mixture for a minimum of 5 minutes. This creates the multilamellar liposomes which are larger than the final desired product (unilamellar liposomes). The next step is the freeze/thaw process. The sample is placed the mixture in dry ice for 5 minutes, and then place it in a 50°C water bath for 5 minutes. This procedure is repeated ten times. At the end of the process, the solution stays in

the hot water bath. Next is the extrusion process where the multilamellar liposomes become the desired unilamellar liposomes, typically 50-250 nm in diameter. The solution is kept at 50°C and extruded through 200 nm pore diameter filter eleven times, ending on the opposite side from where the liposomes began. The final step is gel filtration in which the unilamellar end product is isolated from anything else present in the solution. The separation column is filled with slurry of sephadex and phosphate buffered saline solution. The magneto liposomes are collected in the first fraction from the column during the final separation step. The collected fraction of the magneto liposomes is analyzed via dynamic light scattering resulting a diameter of 150 nm ±30 nm. The TEM image indicates significant amount of nanoparticles inside the liposomes as shown in Figure 4.

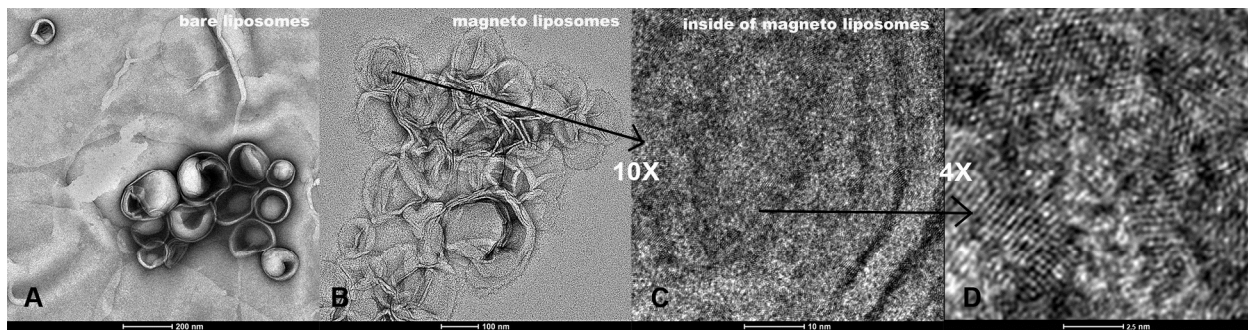


Figure 4 A TEM image of bare liposomes B TEM image of magneto liposomes C TEM image of inside a magneto liposome of image B showing the PtFe nanoparticles D HRTEM image of the PtFe nanoparticles from image C

### AC Impedance measurements

The AC measurements are conducted with potentiostat capable of conducting AC impedance measurements. The electrodes are commercially available carbon printed electrodes using 3 electrode configurations.

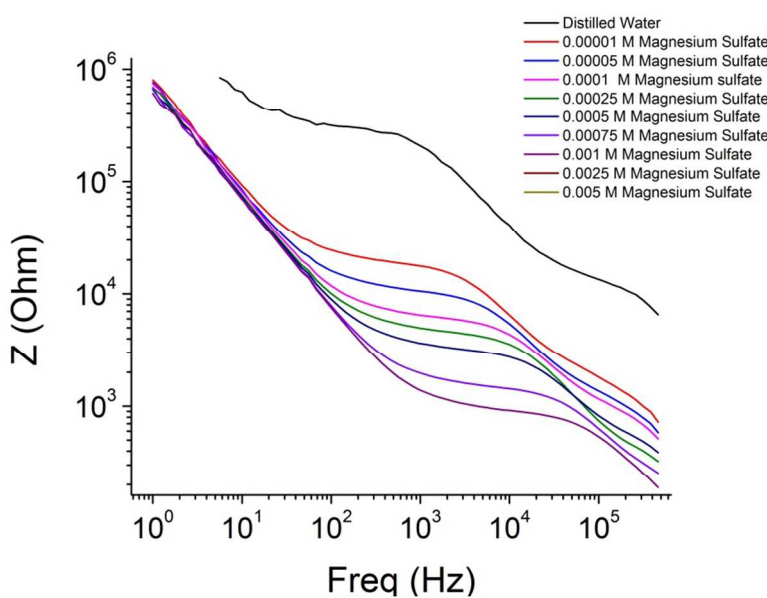


Figure 5 Bode Plot of Magnesium Sulfate at different concentrations

As a first test, the conductivity of  $\text{MgSO}_4$  is tested for different concentrations (Figure 5). Frequency in hertz is displayed on the x-axis and the amplitude of the impedance in ohms is displayed on the y-axis. Impedance is the measure of the maximum volts across the circuit divided by the total current across the circuit, and it is inversely proportional to conductivity. Therefore the lowest concentrations have the highest impedance values because they are the least conductive. The black line represents distilled water which ideally would not have any ions at all. The red line is the lowest concentration of  $\text{MgSO}_4$ . It is only  $1.0 \times 10^{-5} \text{ M}$ , yet there is a significant difference between the impedances of the distilled water and the  $1.0 \times 10^{-5} \text{ M MgSO}_4$ . This demonstrates how sensitive impedance spectroscopy is to low concentrations of ions. As we increase in concentration, we see a decrease in impedance or an increase in conductivity, like expected.

#### 5(6)-Carboxyfluorescein release assay

The model drug of the investigation, 5(6)-Carboxyfluorescein (CF), is responsible for the fluorescence emission from thus prepared liposomes. CF is a hydrophilic fluorescent molecule and it should be entrapped in the core of liposome. CF generates emission fluorescence at around 517 nm. The intensity of CF fluorescence gives the amount of free CF in the system. The change in fluorescence intensity is measured upon exposure to pulsed magnetic field. The fluorescence self-quenching decreases as the CF molecules come out from the liposomes.<sup>24</sup> The steady state

fluorescence is measured at excitation wavelength 460 nm with 1 nm slits. To calculate the drug release from both control liposomes and MLs, 200  $\mu$ L of thus prepared liposomes or MLs is diluted using 3 mL of PBS Buffer. The emission fluorescence spectra of liposomes or MLs before exposing into pulsed magnetic field, after exposing into 10 pulses of pulsed magnetic field and after the addition of 100  $\mu$ L of Triton X-100 are recorded. The addition of Triton X-100 completely releases the CF through vesicles disruption.

## Results and Discussions:

The triggered drug release of the magneto liposomes are tested via the release of conductive  $MgSO_4$  from the liposomes upon exposure to pulsed magnetic fields.

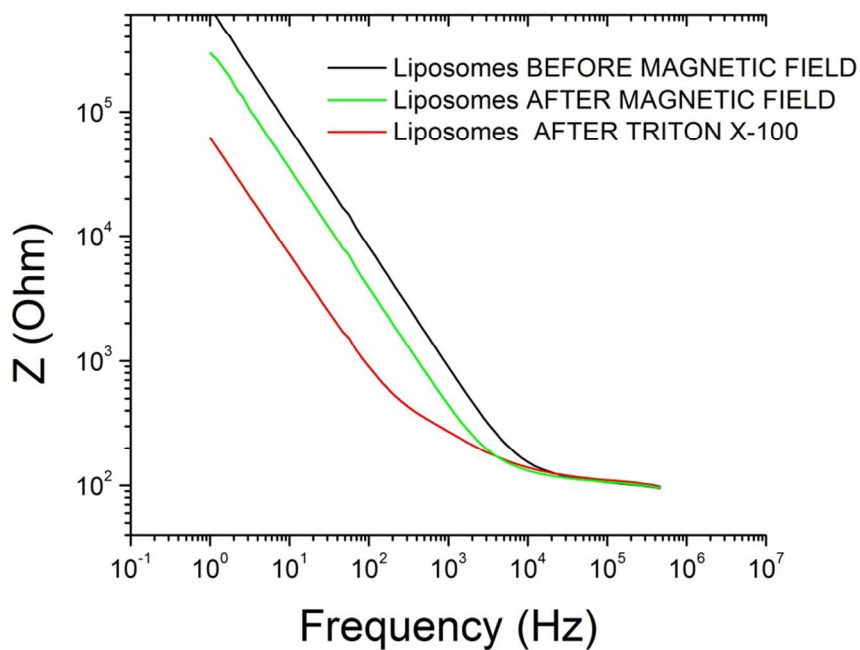


**Figure 6** Bode plot of a magneto liposome solution before and after the application of magnetic fields. Addition of TRITON X-100 destroys the liposomes and releases all the  $MgSO_4$

In Figure 6 another Bode Plot is presented, but this time liposomes and HEPES (4-(2-hydroxyethyl)-1-piperazineethanesulfonic acid) Buffer are in solution. The black line is the liposomes, which contain superparamagnetic nanoparticles and  $MgSO_4$ , mixed with HEPES Buffer. Then the magnetoliposomes were exposed to the strong pulsed magnetic field pulses ten times. The green line represents the magnetoliposomes and HEPES Buffer after exposure to the

magnetic field. As expected there is a decrease in impedance (increase in conductivity) because at least some of the liposomes released their payload of MgSO<sub>4</sub>. The red line is the magnetoliposomes after exposure to Triton X-100. Triton completely destroys all of the liposomes; however, it also contributes to the conductivity. To remove any side effects from the contribution of TRITON X-100 to the overall conductivity, the magneto liposomes are also destroyed with a sonic dismembrator. After the sonication, the sample is left to equilibrate with room temperature for 10 minutes to remove the temperature dependent bias of the conductivity measurement. The results are summarized in Table 1, which shows the MgSO<sub>4</sub> release from magneto liposome after application of 10 magnetic pulses. The individual values show the resistance of the solution at 214 Hz and the concentration of the MgSO<sub>4</sub> is calculated from a formula obtained by fitting the MgSO<sub>4</sub> calibration curve ( $CMgSO_4 = (\sigma - 0.00031)/0.000844^2$ ). Here  $\sigma$  is the conductivity of the sample at 214 Hz expressed in 1/ohm. The control liposomes do not contain magnetic nanoparticles. In addition, to the data presented in the table, experiments are also conducted to assess how many pulses are needed to release the MgSO<sub>4</sub> from the magneto liposomes. Figure 7 shows the impedance measurement of magneto liposome solution following exposure to single magnetic pulses. This measurement indicates that a single magnetic pulse releases a significant portion of the MgSO<sub>4</sub> from the liposome. The magnetic pulses did not produce any noticeable heating of the magneto liposomes.

Table 1 Summary of AC impedance measurements of magneto liposomes exposed to 10 magnetic pulses. The % percentage release is calculated from impedance values at 214 Hz converting them to concentrations.

	Before	After	After	Percent	Average
	Magnetic	Magnetic	Sonication	Release	
	Pulse	Pulses			
Liposome 1	5676	4740	3635	48.5%	47.7+-1.9%
Liposome 2	4786	4325	3782	49.2%	
Liposome 3	5459	4734	3802	45.6%	
Control 1	4129	4177	3496	-1.2%	-9.5+-8.3%
Control 2	3521	3523	3243	-9.5%	
Control 3	3971	3709	3338	-17.8%	

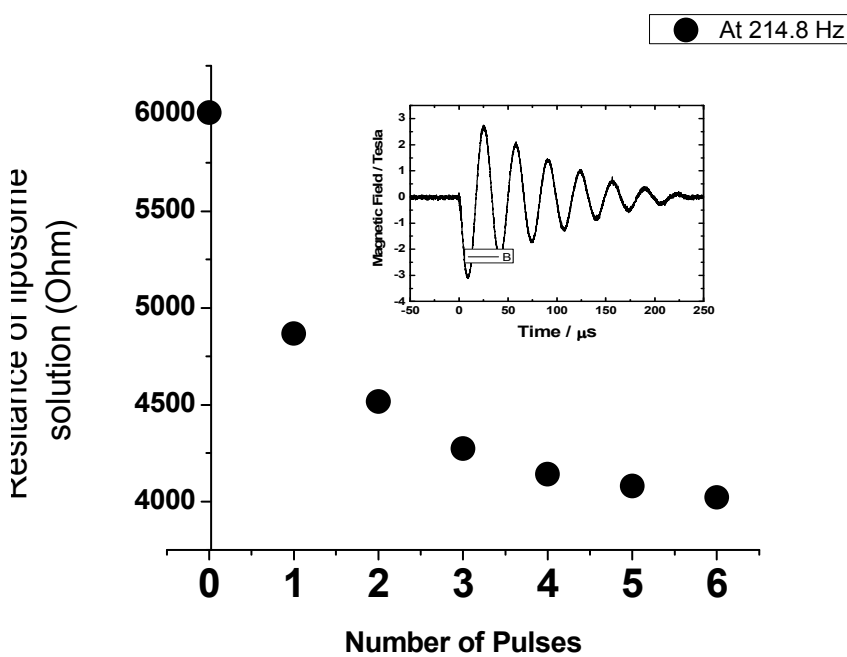


Figure 7 Impedance changes of the magneto liposome solution upon exposure to subsequent magnetic pulses. The magnetic pulses used in the conductivity measurements and its strength is shown in the inset.

### Liposome release studies with 5(6)-Carboxyfluorescein dye

The typical fluorescence emission spectra are shown in Figure 8. Same measurements are performed for other NPs.

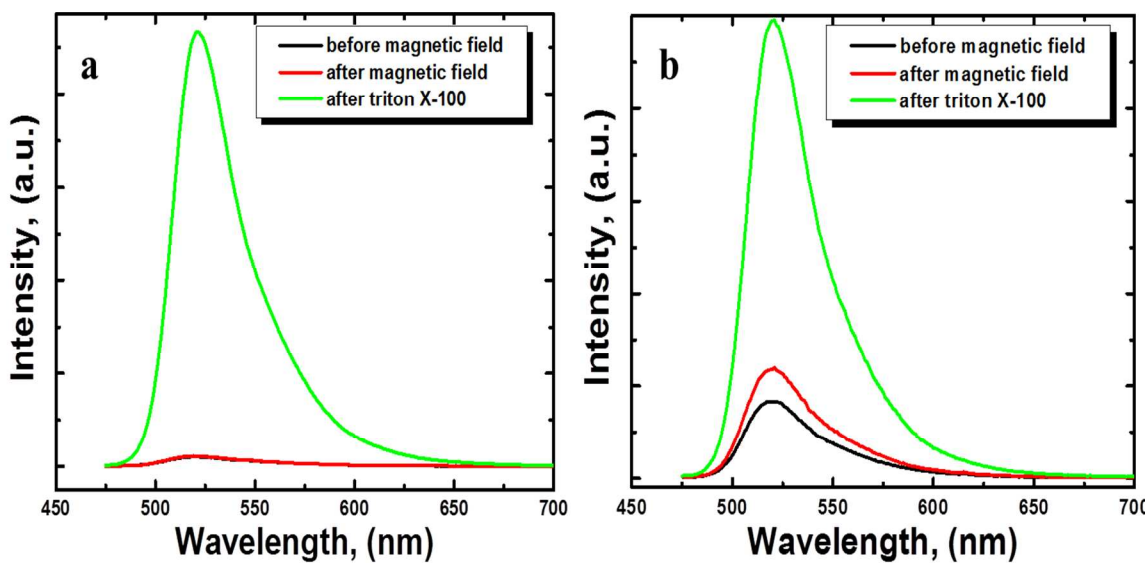


Figure 8 Static fluorescence emission measurements of (a) control liposome, no NP (b) magnetic NPs ( $\text{Fe}_3\text{O}_4$ ) loaded liposome, before/after exposing pulsed magnetic field and after the release of all dye as model drug using Triton X-100.

The clear difference can be seen in the fluorescence emission spectra between the control liposome and magnetic NPs loaded liposome. To quantify the result, percentage release of the drug is calculated. The percentage release of the drug is calculated from the integrated fluorescence intensity of emission spectra. The calculated surface areas under the emission spectra are used to calculate the percentage release as

$$\% \text{ release} = \frac{SA_{AMF} - SA_{BMF}}{SA_{AT} - SA_{BMF}} \times 100$$

where  $SA_{AMF}$  is the surface area after exposing into magnetic field,  $SA_{BMF}$  is the surface area before exposing into magnetic field,  $SA_{AT}$  is the surface area after the addition of Triton X-100. The calculated % releases for control liposomes and  $\text{Fe}_3\text{O}_4$  NPs loaded liposomes are tabulated in the Table 2.

Table 2 Drug release data for control and magnetic NPs loaded liposomes.

Samples	$SA_{BMF}$	$SA_{AMF}$	$SA_{AT}$	% release
Liposome	$1.22 \times 10^6$	$1.27 \times 10^6$	$4.55 \times 10^7$	0.12%
Liposome/ $\text{Fe}_3\text{O}_4$	$2.13 \times 10^6$	$2.96 \times 10^6$	$1.20 \times 10^7$	8.40%

The same experiment is repeated as described above with the hydrophobic, hydrophilic and amphiphilic peptide coated  $\text{Fe}_3\text{O}_4$  NPs, since depending on the surface property of NPs, the position of the NPs in the liposomes is fixed. The % releases of drug are calculated which are given in the following Table 3. The percentage releases with hydrophilic and amphiphilic peptide coated  $\text{Fe}_3\text{O}_4$  NPs are almost same. The percentage release with hydrophobic peptide coated  $\text{Fe}_3\text{O}_4$  NPs is comparatively small. This indicates that the hydrophobic peptide coated  $\text{Fe}_3\text{O}_4$  NPs are not incorporated in the liposomes because of the surface property of NPs.

**Table 3 Drug release data for hydrophobic, hydrophilic and amphiphilic peptide coated  $\text{Fe}_3\text{O}_4$  NPs.**

Samples	$SA_{BMF}$	$SA_{AMF}$	$SA_{AT}$	% release
Hydrophobic	$4.61 \times 10^6$	$4.77 \times 10^6$	$6.95 \times 10^7$	0.24%
Hydrophilic	$5.50 \times 10^6$	$7.28 \times 10^6$	$5.00 \times 10^7$	3.57%
Amphiphilic	$2.77 \times 10^6$	$4.52 \times 10^6$	$5.09 \times 10^7$	3.63%

As it has been shown above, when liposomes, filled with magnetic nanoparticles, are exposed to a short magnetic pulse, model drug molecules are released quickly from the liposomes. In a recent study, Hu *et al*<sup>25</sup> have demonstrated that application of magnetic pulses in the presence of magnetic nanoparticles leads to ultrasound generation. They used the resulting ultrasound for imaging purposes to reconstruct an image of an object filled with magnetic nanoparticles. Their observation is relevant to this work because ultrasound is also commonly used on liposomes to release their content.<sup>26, 27, 28</sup> To explore if ultrasound is generated from our magnetic pulses, iron oxide magnetic nanoparticles were exposed to pulsed magnetic fields. In order to assess accurately if the homogeneous or the inhomogeneous magnetic fields are more effective to generate ultrasound, two electromagnets have been developed that are very similar in construction. The sketch of the first magnet consist of an anti-Helmholtz coil shown in Figure 9 A and B to produce the large inhomogeneous magnetic field on the order of 400 Tesla/meter in a 3 mm center part of the coil. In an anti-Helmholtz coil the winding of the coil pairs are opposing to produce the large inhomogeneous magnetic fields. The second coil (Helmholtz coil) is also prepared with opposite winding that result ~15Tesla homogeneous magnetic field in the full length of the coil (~50 mm). The magnetic field of the Helmholtz coil has been measured by optical method from the Faraday rotation of a small Pyrex rod (Figure 9C). To quantify the

amount of ultrasound the concentration of the nanoparticles is varied inside a glass tube that is attached to a commercially available hydrophone as it is shown in Figure 8D.

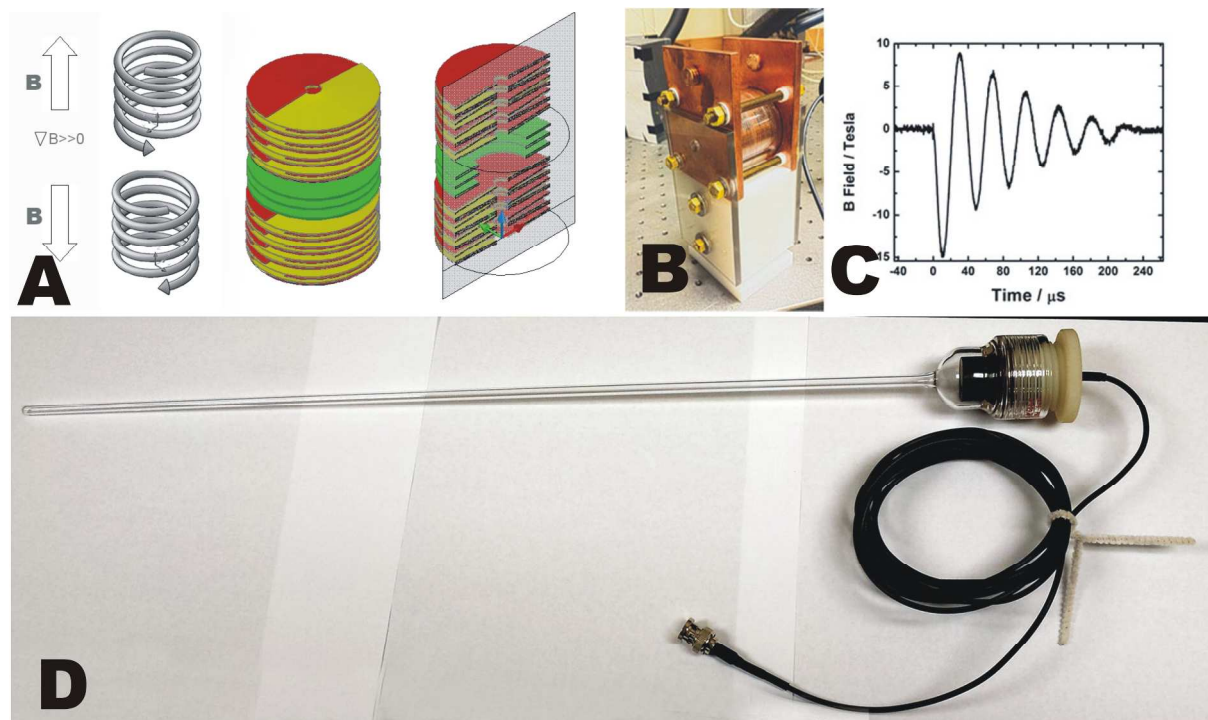


Figure 9 A) Sketch of anti-Helmholtz coil to produce large magnetic field gradient. B) Picture of the finished electromagnet C) Measured magnetic pulse by Faraday rotation of Pyrex glass D) Picture of the experimental apparatus used to detect ultrasound generated from pulsed magnetic fields in the presence of magnetic nanoparticles

In order to accurately assess the amount of ultrasound from the magnet, the signal from the hydrophone is recorded as function of iron oxide concentration including the water as a reference. Figure 9 summarizes the results from the experiments to assess ultrasound generation from magnetic nanoparticles. Figure 10 A) shows that current derivative as function of time along with the hydrophone signal for water and iron oxide magnetic nanoparticle solution. The presented results are for the Helmholtz coil, but very similar results are obtained for the anti-Helmholtz coil as well. The ultrasound power is calculated from the Fourier transform power coefficient of the actual signal. Figure 10 B) shows the Fourier power coefficients for the time dependent signal from water and from iron oxide NP solutions with increasing concentrations. The integrated power coefficients are plotted against the concentration of nanoparticles (shown in Figure 10 C). From these results it is clear that the magnetic nanoparticle generate significant amount of ultrasound whether the magnetic field is homogeneous or inhomogeneous. Ultrasound is commonly used to disrupt the membranes of liposomes; therefore we propose that the ultrasound generation process from the magnetic nanoparticles residing inside the liposomes is

the important underlying mechanism for the disruption of lipid bilayers. The results indicate that both magnet produces ultrasound that is significant compared to the water background at frequencies corresponding to the frequency of the pulsed magnet (~30kHz). In the previous study by Hu,<sup>25</sup> the primary mechanism for ultrasound generation was the linear acceleration of magnetic nanoparticles in the inhomogeneous magnetic fields; however, here we observe that the homogeneous magnetic fields also produce significant amount of ultrasound. It appears that at lower concentrations the inhomogeneous magnetic field has larger contribution to the ultrasound generation (Note that the inhomogeneous magnetic field only impacts 3mm center part of the coil and the homogenous magnetic field affects the entire length of the coil). While Hu et al proposed that only inhomogeneous magnetic fields result in noticeable amount of ultrasound, the data here indicate that homogeneous magnetic fields can also result in ultrasound. The literature indicates<sup>29</sup> that in strong magnetic fields the magnetic nanoparticles form chains of magnetic beads<sup>30, 31</sup> and during this process the displacement of liquid results in ultrasound generation. When the magneto liposomes are exposed to the magnetic fields due to relatively large concentration of magnetic nanoparticles inside the liposome, the generated ultrasound can significantly contribute to the drug release observed under these experimental conditions.

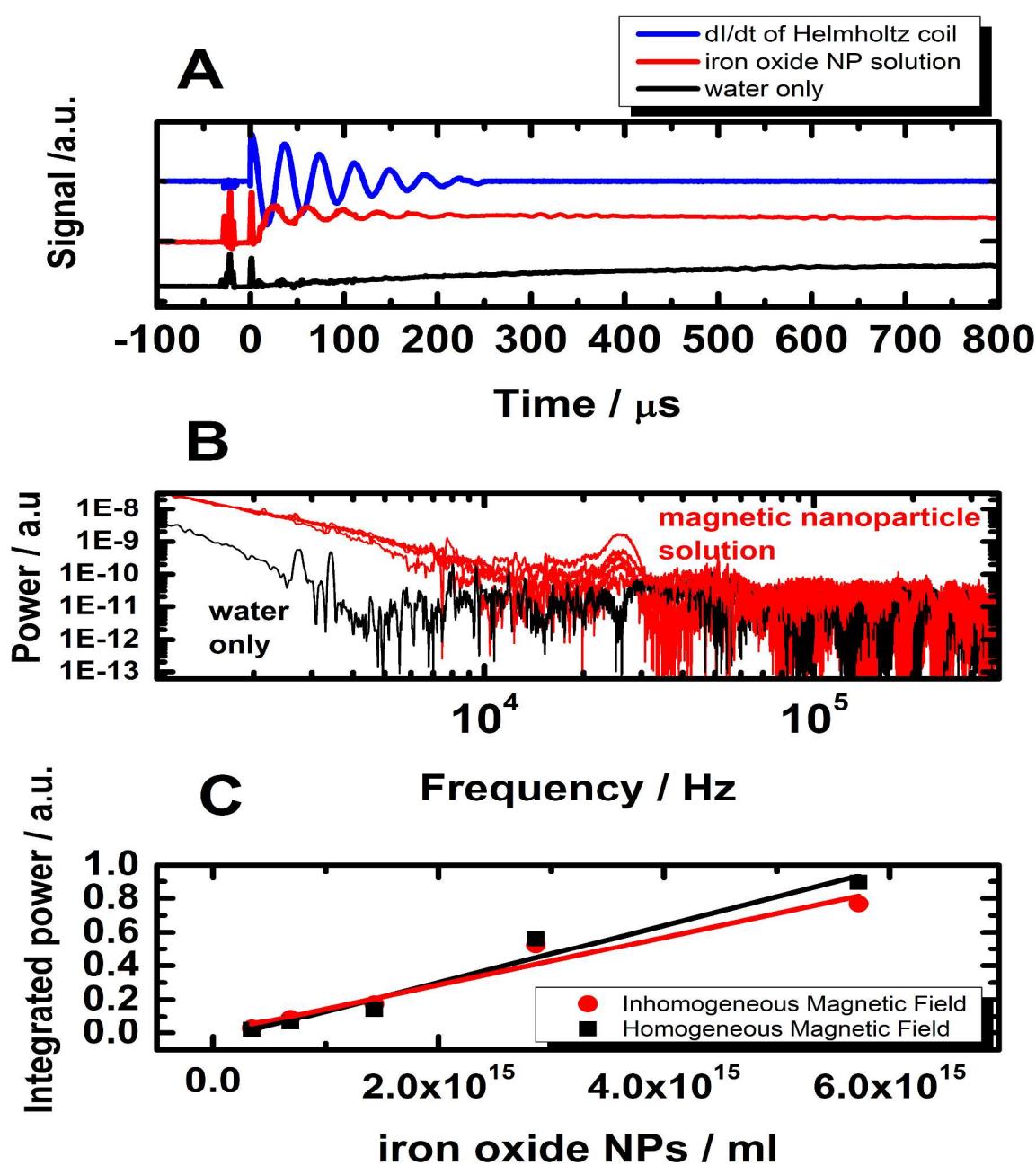


Figure 10 A) Hydrophone signal from iron oxide NP, water in homogeneous magnetic field. As a reference the current derivative of the coil is shown B) Fourier power coefficient of the time dependent signal of the NPs in homogeneous magnetic fields C) Concentration dependence of the ultrasound signal for the homogeneous and inhomogeneous magnetic field. The 100% concentration corresponds to the 0.31 volume% of EMG 607 iron oxide 15 nm in diameter NPs from Ferrotech Corporation

## Summary

Here the fast release of model drug molecules ( $\text{MgSO}_4$  and 5(6)-Carboxyfluorescein) from magneto liposomes loaded with  $\text{Fe}_3\text{O}_4$  NPs or FePt nanoparticles is demonstrated with the help

of strong magnetic pulse(s). The experiments indicate that ultrasound is generated from magnetic nanoparticles in the presence of pulsed magnetic fields, which is proposed to play a key role in the release of the drug molecules from magneto liposomes. The process can be further optimized to maximize the amount of drug lease bases on the solubility of MNPs and the ligand coating of the nanoparticles, but no major difficulty is anticipated.

#### Acknowledgments

The authors would like to acknowledge the support of NSF through grants NSF-930673 and NSF-1128570, and the Terry Johnson Cancer Center at KSU for funding the construction of the pulsed magnet.

**Potential Applications:** 1) Instantaneous delivery of drugs with both temporal and special precision 2) Delivery of therapeutic agents for cancer therapy 3) Delivery of pain killer drug locally following the injection of the drug loaded into magneto liposomes via Intravenous therapy 4) Experimental tool to induce instant repeated physiological changes from drugs therefore allowing kinetic studies in living systems 5) Release of radiation preventive drugs from magneto liposomes induced by the strong electromagnetic field from a nuclear explosion 6) Manipulating/modulating cellular permeability via mechanical force from the pulsed magnetic fields.

## References

1. Bangham, A. D.; Horne, R. W., Negative Staining of Phospholipids and Their Structural  
2. Modification by Surface-Active Agents as Observed in the Electron Microscope. *J. Mol. Biol.* **1964**, *8*, 660-  
3. 8.
4. Gregoriadis, G., Structural Requirements for the Specific Uptake of Macromolecules and  
5. Liposomes by Target Tissues. In *Enzyme Replacement Therapy of Lysosomal Storage Diseases*, J.M.  
6. Tager; G.J.M. Hooghwinkel; Daems, W. T., Eds. North Holland Publishing Company: 1974; pp 131-148.
7. Bangham, A. D.; Hill, M. W.; Miller, N. G. A., Preparation and Use of Liposomes as Models of  
8. Biological Membranes. In *Methods Membr. Biol.*, E.D. Korn, E. P., Ed. Plenum Press: New York, 1974; pp  
9. 1-68.
10. Gregoriadis, G.; Ryman, B. E., Fate of Protein-Containing Liposomes Injected into Rats.  
11. Approach to the Treatment of Storage Diseases. *Eur. J. Biochem.* **1972**, *24*, 485-91.
12. Gregoriadis, G.; Putman, D.; Louis, L.; Neerunjun, D., Comparative Effect and Fate of  
13. Nonentrapped and Liposome-Entrapped Neuraminidase Injected into Rats. *Biochem. J.* **1974**, *140*, 323-  
14. 30.
15. Gabizon, A. A., Applications of Liposomal Drug Delivery Systems to Cancer Therapy.  
16. *Nanotechnol. Cancer Ther.* **2007**, 595-611.
17. Bangham, A. D.; Hill, M. W.; Miller, N. G. A., Preparation and Use of Liposomes as Models of  
18. Biological Membranes. In *Methods in Membrane Biology*, Korn, E., Ed. Springer US: 1974; pp 1-68.
19. Fenske, D. B.; Cullis, P. R., Entrapment of Small Molecules and Nucleic Acid-Based Drugs in  
20. Liposomes. In *Liposomes*, Pt E, Duzgunes, N., Ed. Elsevier Academic Press Inc: San Diego, 2005; Vol. 391,  
21. pp 7-40.
22. Gueven, A.; Ortiz, M.; Constanti, M.; O'Sullivan, C. K., Rapid and Efficient Method for the Size  
23. Separation of Homogeneous Fluorescein-Encapsulating Liposomes. *J. Liposome Res.* **2009**, *19*, 148-154.
24. Martin, F. J.; Gabizon, A.; Huang, S. K.; Papahadjopoulos, D., Sterically Stabilized Liposomes: A  
25. Hypothesis on the Molecular Origin of the Extended Circulation Times. *Biochim. Biophys. Acta, Biomembr.* **1991**, *1070*, 187-92.
26. Moses, M. A.; Brem, H.; Langer, R., Advancing the Field of Drug Delivery: Taking Aim at Cancer.  
27. *Cancer Cell* **2003**, *4*, 337-341.
28. Allen, T. M.; Cullis, P. R., Drug Delivery Systems: Entering the Mainstream. *Science* **2004**, *303*,  
29. 1818-1822.
30. Wang, X., Fabrication and Bio-Application of Functionalized Nanomaterials. In *Fabrication and  
31. Bio-Application of Functionalized Nanomaterials*, Wang, X., Ed. Research Signpost: Trivandrum, Kerala,  
32. India, 2009; pp 121-143.
33. Sparreboom, A.; Kehler, D. F. S.; Mathijssen, R. H. J.; Xie, R.; de Jonge, M. J. A.; de Brujin, P.;  
34. Planting, T.; Eskens, F.; Verheij, C.; de Heus, G., et al., Phase I and Pharmacokinetic Study of Irinotecan in  
35. Combination with R115777, a Farnesyl Protein Transferase Inhibitor. *Br. J. Cancer* **2004**, *90*, 1508-1515.
36. Rozners, E., Non-Ionic RNA Analogs: Stereoselective Synthesis, Biophysical Properties , and  
37. Biological Relevance. *Latv. Kim. Z.* **2006**, *28*.
38. Weissig, V.; Boddapati, S. V.; Cheng, S. M.; D'Souza, G. G. M., Liposomes and Liposome-Like  
39. Vesicles for Drug and DNA Delivery to Mitochondria. *J. Liposome Res.* **2006**, *16*, 249-264.
40. Fritz, H., Pulsed Magnets. *Reports on Progress in Physics* **1999**, *62*, 859.
41. Bartkevicius, S.; Novickij, J., The Investigation of Magnetic Field Distribution of Dual Coil Pulsed  
42. Magnet. *Elektron. Elektrotech.* **2009**, *23*-26.
43. Salaoru, T. A.; Woodward, J. R., Rapid Rise Time Pulsed Magnetic Field Circuit for Pump-Probe  
44. Field Effect Studies. *Rev. Sci. Instrum.* **2007**, *78*.

- 1  
2  
3     20. Mackay, K.; Bonfim, M.; Givord, D.; Fontaine, A., 50 T Pulsed Magnetic Fields in Microcoils. *J.  
4 Appl. Phys.* **2000**, *87*, 1996-2002.  
5     21. Wang, C.; Hou, Y. L.; Kim, J. M.; Sun, S. H., A General Strategy for Synthesizing FePt Nanowires  
6 and Nanorods. *Angew. Chem.-Int. Edit.* **2007**, *46*, 6333-6335.  
7     22. Lacroix, L.-M.; Frey Huls, N.; Ho, D.; Sun, X.; Cheng, K.; Sun, S., Stable Single-Crystalline Body  
8 Centered Cubic Fe Nanoparticles. *Nano Letters* **2011**, *11*, 1641-1645.  
9  
10     23. Basel, M. T., *Targeting Cancer Therapy: Using Protease Cleavage Sequences to Develop More  
11 Selective and Effective Cancer Treatments*. K-State Research Exchange, 2010; Vol. PhD Dissertation.  
12  
13     24. Nappini, S.; Massimo, B.; Francesca, R.; Baglioni, P., Structure and Permeability of  
14 Magnetoliposome Loaded with Hydrophobic Magnetic Nanoparticles in the Presence of a Low  
15 Frequency Magnetic Field. *Soft Matter* **2011**, *7*, 4801-4811.  
16  
17     25. Hu, G.; He, B., Magnetoacoustic Imaging of Magnetic Iron Oxide Nanoparticles Embedded in  
18 Biological Tissues with Microsecond Magnetic Stimulation. *Applied Physics Letters* **2012**, *100*.  
19  
20     26. Dromi, S.; Frenkel, V.; Luk, A.; Traughber, B.; Angstadt, M.; Bur, M.; Poff, J.; Xie, J.; Libutti, S. K.;  
21 Li, K. C. P., et al., Pulsed-High Intensity Focused Ultrasound and Low Temperature Sensitive Liposomes  
22 for Enhanced Targeted Drug Delivery and Antitumor Effect. *Clinical Cancer Research* **2007**, *13*, 2722-  
2727.  
23  
24     27. Huang, S. L.; MacDonald, R. C., Acoustically Active Liposomes for Drug Encapsulation and  
25 Ultrasound-Triggered Release. *Biochimica Et Biophysica Acta-Biomembranes* **2004**, *1665*, 134-141.  
26  
27     28. Schroeder, A.; Kost, J.; Barenholz, Y., Ultrasound, Liposomes, and Drug Delivery: Principles for  
28 Using Ultrasound to Control the Release of Drugs from Liposomes. *Chemistry and Physics of Lipids* **2009**,  
29 *162*, 1-16.  
30  
31     29. Taketomi, S.; Ogawa, S.; Miyajima, H.; Chikazumi, S.; Nakao, K.; Sakakibara, T.; Goto, T.; Miura,  
32 N., Dynamical Properties of Magneto-Optical Effect in Magnetic Fluid Thin Films. *J. Appl. Phys.* **1988**, *64*,  
33 5846-5848.  
34  
35     30. Cutillas, S.; Liu, J., Experimental Study on the Fluctuations of Dipolar Chains. *Physical Review E*  
36 *2001*, *64*.  
37  
38     31. Promislow, J. H. E.; Gast, A. P., Magnetorheological Fluid Structure in a Pulsed Magnetic Field.  
39 *Langmuir* **1996**, *12*, 4095-4102.  
40  
41  
42  
43  
44  
45  
46  
47  
48  
49  
50  
51  
52  
53  
54  
55  
56  
57  
58  
59  
60

